High Nitrate Variability on an Alaskan Permafrost Hillslope Dominated by Alder Shrubs

Rachael E. McCaully[1,2], Carli A. Arendt[1,2], Brent D. Newman[1], Verity G. Salmon[3], Jeffrey M. Heikoop[1], Cathy J. Wilson[1], Sanna Sevanto[1], Nathan A. Wales[1], George B. Perkins[1], Oana C. Marina[1] and Stan D.

[1]Earth and Environmental Sciences Division, Los Alamos National Laboratory, Los Alamos, 87545, United States
[2]Department of Marine Earth and Atmospheric Sciences, North Carolina State University, Raleigh, 27695, United States
[3]Environmental Sciences Division and Climate Change Science Institute, Oak Ridge National Laboratory, Oak Ridge, 37830, United States

Correspondence to: Carli A. Arendt (carendt@ncsu.edu)

Abstract. In Arctic ecosystems, increasing temperatures are driving the expansion of nitrogen (N) fixing shrubs across tundra landscapes. The implications of this expansion to the biogeochemistry of Arctic ecosystems is of critical importance and more work is needed to better understand the form, availability, and transportation potential of N from these shrubs across a variety of Arctic landscapes. To gain insights to processes controlling N within a permafrost hillslope system, the spatiotemporal variability of nitrate (NO_3^-) and its environmental controls were investigated at an alder (*Alnus viridis* spp. *fruticosa*) dominated permafrost tundra landscape in the Seward Peninsula, Alaska, USA. Soil pore water was collected from locations *within* alder shrubland growing along a well-drained hillslope and compared to soil pore water collected from locations *outside (upslope, downslope, and between)* the alder shrubland. Soil pore water collected within alder shrubland had an average NO_3^--N (nitrogen from nitrate) concentration of 4.27 ± 8.02 mg L^{-1} and differed significantly from locations outside alder shrubland (0.23 ± 0.83 mg L^{-1}; $p < 0.05$). Temporal variation in NO_3^--N within and downslope of alder shrubland corresponded to precipitation events, where NO_3^- accumulated in the soil was flushed downslope during rainfall. These findings have important implications for nutrient availability and mobility in N-limited permafrost systems that are experiencing shrub expansion in response to a warming Arctic.

1 Introduction

1.1 Background

Ecosystems in the Arctic are directly and continually impacted by increasing global temperatures (Martin et al., 2008; Chapin et al., 2000; McClelland et al., 2007; Hovelsrud et al., 2011; Schuur et al., 2015), including permafrost degradation with subsequent feedbacks that impact soil moisture, vegetation, and nutrient availability (Shaver and Chapin, 1980; Weintraub and Schimel, 2005; Hinzman et al., 2013; Street et al., 2015; Salmon et al., 2016; Walvoord and Kurylyk, 2016). While there is a clear relationship between climate-induced shifts in vegetation and nutrient abundance, many details remain unknown or

Deleted: Temporal and Spatial
Deleted: n
Deleted: arctic
Deleted: , yet
Deleted: many details about
Deleted: location, and
Deleted: remain unknown
Deleted: address this knowledge gap
Deleted: and edaphic
Deleted: $\delta^{15}N$ and $\delta^{18}O$ of soil pore water were consistent with the predicted range of NO_3^- produced through microbial degradation of N-rich alder shrub organic matter.
Deleted: (
Deleted:)
Deleted: Enrichment of both $\delta^{15}N$ and $\delta^{18}O$ isotopes at wetter downslope locations indicate that denitrification buffered the mobility and spatial extentlimits the mobility of NO_3^--N by transforming it to other N-species.
Formatted: Not Highlight
Formatted: Not Highlight
Deleted: production
Deleted: the effects of
Deleted: ,
Deleted: ,
Moved (insertion) [3]
Deleted: Because of rising temperatures, the Arctic is experiencing
Deleted: ,
Deleted: yet

unpublished about the variability of nutrient availability across- and nutrient mobility within- permafrost systems (Sharkhuu and Sharkhuu, 2012; Barnes et al., 2014; Keuper et al., 2017).

In landscapes with a topographic gradient, NO_3^- contributions in upland areas to surface waters can impact downslope hydrochemistry and alter downstream ecosystems (Vitousek et al., 1997; Koch et al., 2013; Hiltbrunner et al., 2014). Within permafrost landscapes, the mobility potential of nutrients is largely dependent on both the topographic gradient and active layer depth, which also influence soil redox conditions (O'Donnell and Jones, 2006) and vegetation (Ogawa et al., 2006). Previous studies have determined that more research is needed to constrain N-fixing vegetation and topographic controls on NO_3^- mobility in the Arctic (Whigham et al., 2017; Harms et al., 2019; Harms and Ludwig, 2016). Near-surface hydrologic and drainage conditions in permafrost Arctic landscapes are influenced by the seasonal thaw of shallow active layer soils (Romanovsky and Osterkamp, 2000; Yano et al., 2010; Boike et al., 2018). Deeper active layers can result in the growth and expansion of larger plant types (including shrubs) that require drier soils and deeper thaw to accommodate their root systems (Myers-Smith et al., 2011). The phenomenon of shrubs increasing in density and abundance in permafrost landscapes, is known as 'shrub expansion' or 'shrubification' (Tape et al., 2006; Weintraub and Schimel, 2003; Frost and Epstein, 2014; Ju and Masek, 2016; Myers-Smith et al., 2015; Sturm et al., 2001).

Certain shrub genera are more closely associated with climate-induced shrubification than others. *Alnus viridis* spp. *fruticosa* (Siberian alder), for example, is a shrub species (Myers-Smith et al., 2011) that fixes atmospheric nitrogen (N_2) through the symbiotic relationship with *Frankia* bacteria residing within nodules in the alder root systems (Roy et al., 2007). Alders frequently establish on steep hillslopes (Myers-Smith et al., 2011; Tape et al., 2012) and have been associated with elevated concentrations of NO_3^--N in soil pore water in cold environments at high elevations like the Alps (Bühlmann et al., 2014; Hiltbrunner et al., 2014).

The effects of alder on soil chemistry and stream water chemistry have been investigated in alpine and upland systems (Hurd and Raynal, 2004; Bühlmann et al., 2014; Mitchell and Ruess, 2009; Shaftel et al., 2012; Whigham et al., 2017); however, very few of these studies have been conducted in Arctic permafrost landscapes. Rhoades et al. (2001) found that alders in permafrost soils of northwest Alaska influenced soil NO_3^--N and measured high foliar N in various plant types growing within alder understory, suggesting increased soil N below the shrubs. While the linkage between alders and soil N is clear, the variability of soil pore water NO_3^--N in relation to alders, topography, redox conditions, and permafrost in the Arctic has not previously been studied in detail.

1.2 Study objectives

To study the influence of alder on soil chemistry in Arctic permafrost landscapes, we investigated the relationships that exist between N-fixing alders, topography, and soil moisture to determine the dominant controls on NO_3^- availability that occur in

Deleted: how vegetation and nutrient

Deleted: availability in

Deleted: will shift in response to climate change

Deleted: Barnes et al., 2014

Moved up [3]: Because of rising temperatures, the Arctic is experiencing permafrost degradation with subsequent feedbacks that impact soil moisture, vegetation, and nutrient availability (Shaver and Chapin, 1980; Weintraub and Schimel, 2005; Hinzman et al., 2013; Walvoord and Kurylyk, 2016).

Deleted: Hydrologic

Deleted: Near-surface hydrologic conditions and nutrient transport in the Arctic are controlled by the seasonal thaw of shallow active layer soils situated above the permafrost (Boike et al., 2018; Yano et al., 2010). Permafrost degradation alters landscape hydrology (Romanovsky and Osterkamp, 2000) and impacts nitrogen (N) and carbon (C) storage and release (Schuur et al., 2015). Previous and ongoing research demonstrates the linkages that exist between N and C in Aarctic tundraenvironments: both C and N are of critical biological importance in Arctic coastal waters and changing fluxes from Arctic runoff influence primary productivity (McClelland et al., 2007), C to N ratios in Arctic tundra determine response of plant productivity to climate change (Weintraub and Schimel, 2003), and that N likely exerts control on whether C is biogeochemically transformed in reactive catchments, which directly influences carbon-climate feedbacks (Koch et al., 2013). Additional studies (Weintraub and Schimel, 2003; McClelland et al., 2007; Koch et al., 2013; Street, et al., 2015; Salmon, et al., 2016; Ramm et al., 2020) and further emphasize the importance of understanding both changing C and N cyclesavailability and subsequent ecosystem responses in permafrost landscapes.

Moved (insertion) [1]

Deleted: The mobility potential of nutrients across the perm ... [1]

Moved (insertion) [2]

Deleted: in

Deleted: Previous studies have determined that more resear ... [2]

Formatted: Font: Italic

Formatted: Font: Italic

Deleted: microbes

Formatted: Font: Italic

Deleted: nitrate (

Deleted:)

Deleted: permafrost

Moved up [1]: The mobility potential of nutrients across the

Moved up [2]: Inputs of NO_3^- from upland areas into surface

Formatted: Not Superscript/ Subscript

Deleted: ,

Deleted: spatial and temporal

Deleted: production and

permafrost soils situated in a hillslope landscape. We focused our research on a location where a recent study estimated that alder area coverage in the hillslope shrubland community increased by 40% from 7.4 ha in 1956 to 10.4 ha in 2014, with an average rate of alder expansion of 513 m^2 yr^{-1} (Salmon et al., 2019a). Within this field setting, we hypothesize that: 1) NO_3^- availability varies both spatially and temporally on short scales across permafrost landscapes; 2) proximity to alder shrublands is a dominant control on NO_3^- availability in soil pore water and will be highest within and immediately downslope of alder stands; and 3) NO_3^- mobility is limited by changes in redox conditions across the hillslope topographic gradient.

2 Materials and methods

2.1 Study location

Approximately 80 km north of the Alaskan coastal town of Nome and 12 km east of Mary's Igloo, the research hillslope of interest is located at mile marker 64 of Kougarok Road (65°09'50.1"N, 164°49'34.2"W) and is referred to as the Kougarok Hillslope (KG Hillslope; Fig. 1). KG Hillslope is a prominent hillslope (elevation from 40-140 m.a.s.l.) with the Kuzitrin River to the north and west (~ 11° topographic slope) and a series of shallow thermokarst lakes to the east (~ 5° topographic slope). The site is composed of metagranitic Late Proterozoic bedrock outcropping at the top of the hill (Hopkins et al., 1955), and gives way to continuous permafrost on the lower slope which is likely Quaternary aged sediments composed of peat, alluvial sediment, and interlaced gravel lenses (Hopkins et al., 1955; Till et al., 2011). The hillslope is asymmetrical and slopes more steeply to the west than to the east (~ 11° and ~ 5° topographic slope, respectively). The KG Hillslope is overlain by an active soil layer containing organic peat and mineral horizons (taxonomic soil classification not available) and is well drained in the upland area due to topographic gradient.

Vegetation found in the upland area primarily includes alder growing in a densely populated alder shrubland community near the crest of the hill interspersed by lichen, moss, and dwarf shrubs. Vegetation in the lowland area is characterized by either alder savanna or tussock tundra plant communities (Iversen et al., 2016; Salmon et al., 2019b). The term 'alder savanna' was defined by Frost et al., (2013), who stated, 'Such shrubland communities, colloquially referred to as 'alder savannas', have been described at several locations in Low Arctic and interior montane Alaska (Racine 1976, Racine and Anderson 1979, Chapin et al., 1989). Regular spacing of alders in 'alder savannas' has been attributed to intra-specific competition for limiting nutrients (Chapin et al., 1989).'

Areas defined as *alder shrubland* communities are dominated by large stands that are exclusively alder and thrive on steep hillslopes (Tape et al., 2006, 2012; Salmon et al., 2019a-b). Whereas, *alder savannas* occur in weakly developed water tracks and consist of short alder dispersed with other deciduous shrub species and graminoids. Between the lowland alder savanna water tracks, tussock tundra plant communities lack alder and are characterized by graminoids (E.g. *Eriophorum vaginatum* and *Carex bigelowii*), dwarf shrubs (E.g. *Betula nana* ssp. *exilis*), lichens (E.g. *Cladonia* spp.) and moss (E.g. *Sphagnum* spp.).

Deleted: on

Deleted: This study was conducted as part of Next Generation Ecosystem Experiments - Arctic (NGEE - Arctic), a U.S. Department of Energy (DOE) project that informs Earth System Models (ESM) through the collection and incorporation of experimental data in the face of increasing Arctic temperatures.

Deleted: (with proximity to alders)

Deleted: (daily and seasonally)

Deleted: are the dominant source of

Deleted: to

Deleted: through mineralization and nitrification of organic matter derived from alder leaf litter and woody material

Deleted: buffered

Deleted: .160714

Deleted:

Deleted: -

Deleted: .

Deleted: 828275

Deleted:

Deleted: a-b

Deleted: write

Deleted: It is important to note that the

Formatted: Font: Italic

Deleted: are

Deleted: , which

Deleted: A

Formatted: Font: Italic

Formatted: Font: Italic

Formatted: Font: Italic

Formatted: Font: Italic

Formatted: Font: Italic

Formatted: Font: Italic

Formatted: Font: Italic

A co-located study by Salmon et al. (2019a-b) defines the vegetation parameters of the hillslope in further detail including alder stand height, basal area and nodule biomass per shrub and per ground coverage. Active layer soils are deeper in the lowland area than the upland area soils, have a thicker organic peat horizon, and are poorly drained due to low topographic gradient (Salmon et al., 2019a-b). The lowland is frequently saturated in inter-tussock areas, especially at the slope break between the steep upland area and shallow lowland area, and within the alder savanna community.

For our study, soil pore water compositions within alder shrubland in the upland area were compared to soil pore water compositions outside alder shrubland (both in upland and lowland areas; see Fig 1). These samples were collected over four field campaigns with a higher-resolution focus and additional monitoring at two alder patch transects (A1 and A4) during the latter campaigns (Fig. 1; Fig. 2). The A1 transect includes a sampling location we identify as a 'seep', which is a direct seep from the ground located at the slope transition between upland and lowland zones (Fig. 1b). The volume of water sourced from this seep was too small to measure directly but is estimated to be < 2 cm^3 s^{-1}. However, water actively trickled from this seep location during all sampling campaigns and is likely representative of active layer melt that surfaced at the upland-lowland transition.

2.2 Sample design

To investigate the aforementioned hypotheses, this study was subdivided into two phases: an initial phase to identify NO_3^--N 'hotspots' in relation to the alder shrubland community (Phase 1) and a comprehensive informed phase (Phase 2) to further address each of the three hypotheses. Phase 1 (July 18-21, 2017) consisted of a synoptic survey to establish soil NO_3^--N variability within and adjacent to five upland alder shrubland areas (A1 – A5; Fig. 1a). To capture this variability, transects were installed with sampling points located within alder shrubland as well as upslope and downslope of the shrubland. These transects also captured the transition between upland and lowland landscape position, which was determined to be located at the most downslope extent of each alder shrubland area.

Phase 2 (September 14-16, 2017, July 22-27, 2018 and September 21-22, 2018) sampling addressed the variability of NO_3^--N within and downslope of two of the alder shrubland areas (A1 and A4 transects; Fig. 1b) that were exposed to the same topographic and climatic conditions and examined this variability with respect to topographic gradient. The A1 and A4 transects are located at similar relief on the eastern slope near the crest of the KG Hillslope; however, the transects extend through and downslope of two separate alder patches allowing the nutrient dynamics associated with each shrubland area to be examined independently. These transects were examined with increasing resolution throughout sampling campaigns to determine NO_3^--N variability within the shrubland and to capture the extent of NO_3^- availability down gradient of the shrubland (see Table S5 in the Supplemental material for further details of the number of sampling locations per transect for each campaign). To address these spatiotemporal controls, we measured soil pore water NO_3^--N concentrations within, between, and downslope of alder shrubland, and measured the natural abundance of redox sensitive species (including manganese (Mn)

Deleted: (refer to Salmon et al., 2019a-b for a complete description of plant communities at this site).

Deleted: temporally

Deleted: , and spatially from five transected alder patches and two lowland transects,

Deleted: of the

Deleted:

Deleted:)

Deleted: Two additional transects were established along the eastern slope of the lowland area to capture nutrient availability in both the alder savanna and tussock tundra communities: 1) a Road Transect that was parallel to and ~5 m from the road, and 2) a Middle Transect that was 400-m upslope of and parallel to the road transect (locations shown in Fig. 1b).

Deleted: spatiotemporal

Deleted: (Fig. 1c)

Deleted: se two

Deleted: spatial and temporal

Deleted: $\delta^{15}N\text{-}NO_3^-$ and $\delta^{18}O\text{-}NO_3^-$

ferrous iron (Fe^{2+}), and sulfate (SO_4^{2-})) along the transects to assess biogeochemical processes and controls on nutrient availability in soil pore water across the tundra. Although an important intermediate form of nitrogen, NH_4^+ was measured but is not discussed with detail in this study due to low dissolved concentrations in these pore water samples (Table S1; Supplemental material).

Soil pore water and bulk soil samples were collected from each sampling location to assess NO_3^--N concentrations and any correlations with soil moisture. In Phase 1 (the July 2017 campaign), samples were collected at each of the five alder patches (Fig. 1a). In Phase 2, which spanned the three subsequent sampling campaigns, all samples were collected from the A1 and A4 transects (Fig. 1b), with the goal of examining spatial NO_3^--N variations with higher resolution. The alder stand along the A1 transect covers roughly ~3,400 m^2 in area and is located 20 m north of the A4 transect, which intersects an alder stand covering roughly ~6,400 m^2 in area (Fig. 1b). Sample collection evolved from three sampling locations per transect in Phase 1 to sampling locations placed every 10 m along each transect in Phase 2, initiating within the alder shrubland and terminating 50 m downslope from the bottom of each shrubland area (Fig. 1b). The number of samples per location for each sampling campaign varied as spatial resolution increased through time and are shown in the associated Tables S4 and S5 in Supplemental material.

2.3 Soil pore water

Soil pore water samples are the basis of our NO_3^-N availability and variability investigation and were collected by installing a nest of macro-rhizons at each sample location (Rhizosphere Research Products; hereby referred to as rhizons) using the methods described by Seeberg-Elverfeldt et al., (2005). Rhizons were installed at depths between 15-30 cm, and due to the volume required for chemical analyses, were installed in nests (on average 5 rhizons per nest) at each sampling location depending on soil saturation and water availability. Soil pore water was collected in 60- ml syringes connected by luer-lock mechanisms on each rhizon. Syringes were subsequently combined into one sample per nest to obtain adequate volumes for analyses and ensure a homogenous bulk sample. Syringes were re-hung from rhizons at their respective sampling locations and left overnight before collection the next morning.

After the soil pore water collected from each nest was integrated for a representative sample, the samples were then filtered, frozen, and transported to Los Alamos National Laboratory's Geochemistry and Geomaterials Research Laboratory (GGRL) where they were stored frozen until undergoing geochemical analysis. Cations were measured using inductively coupled plasma optical emission spectrometry (ICP-OES) on a Perkin Elmer Optima 2100DV instrument (Perkin Elmer Inc., USA) using United States Environmental Protection Agency (EPA) method 200.7; precision is justified to 0.01 mg L^{-1}. Anions were measured with ion chromatography on a Dionex ICS-2100 instrument (Thermo Fisher Scientific Inc., USA) utilizing EPA method 300 (Throckmorton et al., 2015); precision is justified to 0.01 mg L^{-1}. Isotopic analyses including $\delta^{15}N$ and $\delta^{18}O$ of

Deleted: determine
Deleted: sources of NO_3^- and
Deleted: such as denitrification occurring in
Formatted: Superscript
Formatted: Subscript
Formatted: Superscript
Deleted: measured
Deleted: ry
Deleted: M
Deleted: The number of samples per location for each sampling period are shown in Supplementary Material.
Deleted: 1b
Deleted: 1c
Deleted: spatial and temporal
Deleted: through a tighter lens
Deleted: shrubland
Deleted: has
Deleted: shrubland
Deleted: 1c
Deleted: 1c
Deleted: (See Supplementary Material for additional details)
Formatted: Space Before: 0 pt, After: 0 pt
Deleted: T
Deleted: to measure major ion concentrations and isotopic compositions
Formatted: Not Highlight

soil pore water and soil pore water NO_3^--N was also performed to gain insights to nitrate sources and likely biogeochemical processes occurring in our study location (see associated Supplemental material for full details).

2.4 Soil and leaf litter

Soil and leaf litter samples were collected for comparison to soil pore water NO_3^--N content and to assess possible correlations between parameters. Along the A1 and A4 transects, soil was collected for soil moisture analysis from 15-cm depths (and at 30-cm depths where soil was deep enough) in pre-weighed tins, sealed with parafilm, and frozen for preservation. Samples were not collected shallower than 15 cm depth because of the large presence of peat biomass at shallow depths and because all soil pore water samples were collected from ≥15 cm depths. A total of 27 soil samples were collected during July 2017, 6 during September 2017, and 24 in July 2018.

In July 2018, three soil pits (P1, P2, and P3) were dug and described along the A1 transect (Fig. 1b). In each pit, soil was excavated to frozen soil, verified by presence of ice and sub-freezing soil temperatures. Soil was collected at an interval of 20 cm in each pit. Pits 3 and 1 had total depths of 46 cm and 55 cm to frozen soil, respectively, and soil samples were collected at 20 cm and 40 cm. Pit 2 had a depth of 61 cm to frozen soil and soil samples were collected at 20-, 40-, and 60-cm depths. All soil samples were frozen and transported to GGRL or North Carolina State University Department of Marine, Earth, and Atmospheric Sciences in Raleigh, North Carolina where they were stored frozen until analysis (See Supplemental material for additional details).

Alder leaf litter was collected in September 2018 from six locations along the A1 and A4 transects (3 samples from each transect), stored in sealed plastic bags, frozen, and homogenized prior to analysis (n=6). A contamination issue occurred with one of the leaf litter samples collected from the A4 transect, leaving us with n = 5. Thirteen soil samples and five leaf litter samples were analyzed for total N, $\delta^{15}N$ of soil organic nitrogen (SON) and C/N ratios (O'Donnell and Jones, 2006; Moatar et al., 2017; See Supplemental material for additional details).

2.5 In situ parameters

In-situ parameters were measured for each water sampling location to provide insights to environmental field conditions, including depth to frozen soil or bedrock, soil temperature at rhizon sampling depth (~15 cm), soil pore water pH, dissolved oxygen (DO), and specific conductivity. Summaries of DO, pH, and conductivity are provided in Table S2 (Supplemental material); no significant correlations with NO_3^--N were observed (r^2 = 0.02, 0.2, 0.06, respectively). Iron (Fe) speciation parameters were collected for two days during the July 2018 field campaign. These were mixed with ferrozine (to fix Fe^{2+} for later analysis) on-site and subsequently analyzed at GGRL using the Fe-ferrozine method (Stookey, 1970). The Fe speciation

Deleted: Isotopic values are reported in delta (δ) notation as the deviation from an established standard in units per mil (‰). Isotopic data for $\delta^{15}N$ and $\delta^{18}O$ of soil pore water and soil pore water NO_3^--N were measured using the methods outlined in Heikoop et al., (2015); precision is justified to 0.1 ‰. A modified denitrifier method outlined by Sigman et al., (2001) and Casciotti et al., (2002) was used and analyses were made using a GV Isoprime isotope ratio mass spectrometer (IRMS) coupled to a TraceGas peripheral instrument (See Supplementary Material for additional details). ¶
¶
The production of NO_3^- through nitrification is a microbially mediated process that produces predictable isotopic compositions through kinetic fractionation (Kendall and McDonnell, 1998). Based on the assumption that microbial nitrification utilizes two oxygen (O) atoms from water (H_2O) and one O atom from the atmosphere (O_2), the expected range of $\delta^{18}O - NO_3^-$ derived from microbial nitrification (Kendall and McDonnell, 1998) was calculated using Eq. (1): ¶
$\delta^{18}O - NO_3^- = \frac{2}{3}(\delta^{18}O - H_2O) + \frac{1}{3}(\delta^{18}O - O_2)$, ... (1)¶
where atmospheric $\delta^{18}O$-O_2 is +23.5 ‰ (Kendall and McDonnell, 1998). Isotopic data for $\delta^{18}O$ - H_20 was measured directly from soil pore water samples using a GV Instruments Multiflow peripheral instrument (Heikoop et al., 2015). The concentration of dissolved organic nitrogen (DON) was calculated as the difference between total dissolved nitrogen (TDN-N) (measured using persulfate oxidation) and NO_3^--N (Eq. (2), assuming negligible concentrations of other inorganic N species), and the range of $\delta^{15}N$-DON was derived using Eq. (3).¶
$[DON] = [TDN] - [NO_3^-]$, ... (2)¶
$\delta^{15}N_{DON} = \frac{(\delta^{15}N_{TDN} \times [TDN]) - (\delta^{15}N_{NO3} \times [NO_3^-])}{[DON]}$, ... (3)

Deleted: At each sampling location

Deleted: 1c

Deleted: ry

Deleted: Material

Deleted: five

Deleted: 5

Deleted: ry

Deleted: M

Deleted: e

Deleted: and

Deleted: ed

Deleted: ry

Deleted: Material

method determined Fe^{2+} and total Fe (Fe_{Total}; Stookey, 1970). Fe^{3+} was later calculated as the difference between Fe^{2+} and Fe_{Total}.

2.6 Statistical analyses

Data collected had normal distribution and no outliers were identified. Thus, all measurements are included in the statistical analyses. Nonparametric Mann-Whitney rank sum tests were performed (Helsel and Hirsch, 2002) to identify significant differences between geochemical signatures - specifically NO_3^--N, Fe^{2+}, Fe_{Total}, Mn, and SO_4^{2-} - of soil pore water within the alder shrublands and outside the alder shrublands in Phases 1 and 2 (see Supplemental material). The Mann-Whitney statistical analyses performed quantified the spatial variability between upland (alder shrubland) and lowland (alder savanna) regions of our A1 and A4 transects collected during the July 2018 and September 2018 field campaigns and did not factor in temporal variability as our time-series were limited. The individual rhizon nests that composed the upland and lowland sampling sites are defined in Supplemental Table S5 and the detailed outcomes of the Mann-Whitney tests performed are provided in Supplemental Table S6. P-values less than 0.05 were considered statistically significant. Simple linear regressions were used to determine relationships between NO_3^--N and variables including soil moisture, depth to frozen soil or bedrock, and Fe. To directly compare the variability within each chemical compound across the KG Hillslope, the coefficient of variation (Brown, 1998) was calculated for calcium (Ca), sodium (Na), chloride (Cl^-), and NO_3^--N by dividing the standard deviation of the population by the population mean (Table S3, Supplemental material). Ca, Na, and Cl^- are all compounds that typically have low variability within the environment. Consistently high coefficient of variation of NO_3^--N (> 1.5) and low ratios of Ca, Cl^-, and Na (< 1.5) indicate additional (biological) processes acting on NO_3^--N production. MATLAB R2017a was used for all statistical analyses and figure generation.

Deleted: ry

Deleted: M

Deleted: T-tests were performed to identify significant differences between $\delta^{18}O$ during each season.

Deleted: ry

Deleted: M

3 Results

3.1 Soil depth and moisture

Soils within each upland patch were similar in composition with general defining characteristics of a surficial peat horizon underlain by decayed peat and a transitional horizon into mineral soil at a depth of ~12 to ~15 cm, followed by bedrock or frozen soil (personal observations of field participants; Salmon et al., 2019a-b). Soil composition, moisture, and active layer depth within the lowland portion of the A1 and A4 transects were similar but differed from the upland portion of the transects (Table S4; Supplemental material). During both Phase 1 and Phase 2, the mean gravimetric soil moisture content (percent dry/wet weight) was lowest in the upland area (28.5%, 28.4%, and 36.6% in July 2017, September 2017, and July 2018 respectively) and greatest in the lowland area (>50%). The lowlands were inundated during the Phase 2 September 2017 campaign and contained standing water in various inter-tussock locations during the July 2017 and July 2018 sampling campaigns. The mean depth to bedrock or frozen soil was greater in the lowland area (mean of 56.5 cm and 54.3 cm in September 2017 and July 2018 respectively) than the upland area (mean of 45.7 cm and 36.6 cm in September 2017 and July

Deleted: ,

Deleted: other

2018 respectively) during all but one sampling campaign (July 2017; Table S4; in Supplemental material). Soil moisture content and depth to bedrock or frozen soil were not measured during the September 2018 (September 21-22) sampling campaign due to logistical and sampling challenges.

3.2 Phase 1: initial results from five alder patches

From July 18-21, 2017 soil pore water NO_3^--N concentrations were significantly higher ($p < 0.01$) within the alder shrubland than sampling locations upslope and downslope of the shrubland along the A1, A2, A3, and A5 transects (Fig. 2a; additional details in Supplemental material). A brief precipitation event (with a high of ~13° C) occurred overnight on July 18th (Western Regional Climate Center, 2017) but unfortunately the field site rain gauge was out of commission and there is not a quantitative rain amount for this event. Parameters including soil depth, moisture content, pH, dissolved oxygen, and conductivity did not have apparent controls on NO_3^--N and are reported in Tables S2 and S4 in Supplemental material. Soil pore water NO_3^--N was initially negligible within the A1 alder shrubland (Fig. 3a) but increased in concentration following the rainfall event. A similar increase in NO_3^--N was also observed at a seep located at the transition between the upland and lowland along the A1 transect on 19 July relative to the other sampling days from the initial July 2017 sampling campaign. This seep is likely representative of water flowing directly from within the A1 alder shrubland to the lowland area (Fig. 2b), perhaps through fractured bedrock. Phase 1 results show that soil pore water NO_3^--N was elevated both from one alder shrubland patch to another (ranging from 0.3 mg L^- to >10 mg L^-) and within alder shrubland relative to other sampling locations along each transect. The four-day sample collection along the A1 transect revealed daily variations in NO_3^--N availability at our sampling locations (0.51 to 10.08 mg L^{-1}) likely associated with observed rainfall. Both the Road and the Middle transects located in the lowland tussock tundra and alder savanna communities had low NO_3^--N (< 1.0 mg L^{-1}).

3.3 Phase 2: NO_3^--N variability between two alder patches

3.3.1 September 2017

During the 2017 September sampling campaign (September 14-18), conditions were cool (high of ~5.4° C), with daily precipitation (personal observation of field participants; Western Regional Climate Center, 2017). NO_3^--N was elevated within the A4 shrubland and downslope of the A1 shrubland (Fig. 3b), but negligible in soil pore water collected from upland areas between the two transects. The mean NO_3^--N concentration within the A1 and A4 transects did not vary significantly from the mean NO_3^--N concentration directly downslope of the alder shrubland ($p > 0.05$; reference purple sampling locations in Fig. 1b). However, the mean concentration of NO_3^--N both within and directly downslope of the shrublands was significantly greater ($p < 0.05$; Table S4 in Supplemental material) than the mean NO_3^--N concentration of the Middle and Road transects in the furthest extent of the lowland area (Transects M and R in Fig. 1a), indicating that transport potential of NO_3^--N is limited to near the slope break.

Deleted:). (
Deleted: S
Deleted: ry
Deleted: M
Deleted: synoptic
Deleted: ,
Deleted: was significantly greater
Deleted: ry
Deleted: M
Deleted: tmospheric conditions were mild (high of ~13° C) and a
Deleted: ry M
Deleted: all other sampling days
Deleted: 58.61
Deleted: and wet
Deleted: The A1 and A4 transects were examined in greater detail by increasing the spatial resolution of soil pore water chemistry sampling (Fig. 1c).
Deleted: shrublands
Deleted: (
Deleted: ; Supplementary Material
Deleted: ry
Deleted: M
Formatted: Not Superscript/ Subscript
Deleted: .

3.3.2 July 2018

During the 2018 July sampling campaign (July 22-26), NO_3^--N was elevated along the A1 and A4 transects (Fig. 2b and Fig. 3c), both within the shrubland and up to 20-m downslope of the shrubland, where the transition between upland and lowland occurs (Fig. 3c). Each of the five sampling days in July were dry (no precipitation, high of ~16° C), and no notable temporal variation (< 3 mg L^{-1} difference) in NO_3^--N was observed along the A1 and A4 transects (Fig. 4a-b). NO_3^--N concentrations measured from two soil pits located along the A1 transect also increased with depth (Table S5, Supplemental material). Despite the dry conditions, we directly observed water seeping from the upslope wall into each pit, suggesting that interflow was actively occurring across the A1 transect from the upland to lowland areas. Nitrate-N concentrations decreased from upland to lowland along both the A1 and A4 transects (significantly different at $p < 0.001$; Table S5, S6 in Supplemental material). This pattern was mirrored by Fe, which increased in concentration from upland to lowland ($p < 0.001$) along each transect (Fig. 4b and Table S5, S6 in Supplemental material). Similarly, Mn increased from the upland to lowland along the A4 transect ($p < 0.05$; Fig. 4b and Table S5, S6 in Supplemental material). Spatial trends in Mn were not identified, however, along the A1 transect (Fig. 4a) with respect to Mn reduction ($p > 0.05$; Table S5, S6 in Supplemental material). No trends or significant difference ($p > 0.05$) in SO_4^{2-} concentrations were observed along the A4 transect (Table S5, S6 in Supplemental material).

3.3.3 September 2018

In September 2018 (21-22), similar patterns in NO_3^--N concentration occurred along both A1 and A4 transects (Supplemental material), with the highest NO_3^--N at locations within and directly downslope of the shrubland. Total Fe and SO_4^{-2} did not vary along the A1 transect, but Fe_{Total} increased along the A4 transect and SO_4^{-2} increased between 0-20 m downslope of the alder shrubland (Table S5, Supplemental material). Manganese was negligible (< 0.01 mg L^{-1}) along both A1 and A4 transects. No precipitation events occurred during sampling in September 2018.

4 Discussion

4.1 Sources of nitrate

Previous studies conducted in continuous, polygonal permafrost areas without alders indicate that soil moisture is the dominant control on NO_3^- production (Heikoop et al., 2015). However, at the KG Hillslope where polygonal permafrost features do not exist and the landscape is controlled by slope gradient rather than microtopography, no direct relationship was observed between and NO_3^--N and soil moisture ($r^2 < 0.2$; Fig. S1 in Supplemental material). Instead of being associated with soil moisture, at this site, NO_3^--N concentrations were tightly constrained by the presence of alder shrublands. Although NO_3^--N was generally absent in the poorly drained (wet) lowland area, it was elevated within alder patches on the well-drained (dry) upland area. Elevated NO_3^--N was not observed laterally adjacent to or upslope of alder shrubland. Therefore, while soil moisture likely plays a role in determining NO_3^--N availability, our results indicate that the alder shrubland community was the dominant control on NO_3^--N availability in soil pore water on the KG Hillslope. Furthermore, Darrouzet-Nardi and

Deleted: ry
Deleted: M
Deleted: ry
Deleted: M
Deleted: ry
Deleted: M
Deleted: ry
Deleted: M
Deleted: ry
Deleted: M
Deleted: ry
Deleted: M
Deleted: ¶
Deleted: ry
Deleted: M
Deleted: ry
Deleted: M
Deleted: **3.4 Isotopes of nitrate and water**¶
A total of 62 soil pore water samples from locations within and downslope of alder shrubland had sufficient NO_3^- concentrations (> 0.5 mg L^{-1}) to measure $\delta^{15}N$ and $\delta^{18}O$ of NO_3^- across all four sampling campaigns (Fig. 5; more details in Supplementary Material). Generally, $\delta^{15}N - NO_3^-$ at lowland locations downslope of the alder shrubland were more enriched than locations within alder shrubland, and high $\delta^{18}O - NO_3^-$ values correspond to high $\delta^{15}N - NO_3^-$ values at the downslope locations (Fig. 5). Because minimal fractionation takes place during N_2 fixation, NO_3^- produced by mineralization and nitrification of organic matter derived from fixation (alder leaf litter) should have $\delta^{15}N$-NO_3^- in the range of -5.0 ‰ to 5.0 ‰ (Kendall and McDonnell, 1998). $\delta^{15}N$ of leaf litter N (n=10) collected from the shrubland along all five transects (along with $\delta^{15}N$ data from Salmon et al., 2019b; n=5) ranged from -2.8 ‰ to -0.9 ‰. $\delta^{15}N$ of total dissolved nitrogen (TDN) ranged from -11.3 ‰ to -0.9 ‰, and $\delta^{15}N$ of dissolved organic nitrogen (DON) ranged from -19.1 ‰ to -8.0 ‰ (calculated values, see Section 2.3). $\delta^{15}N$ of soil organic nitrogen (SON) ranged from 0.5 ‰ to 3.6 ‰ (n = 13). Atmospheric NO_3^- values of $\delta^{15}N$ range from ~ -15 ‰ to ~ +15 ‰ and $\delta^{18}O$ ranging from ~ +60 ‰ to ~ +94 ‰ (Granger and Wankel, 2016). A summary of $\delta^{18}O$ compositions is provided in Supplementary Material (Table S7).¶
Deleted: ry
Deleted: M
Deleted: production

Weintraub (2014) found evidence for spatial inaccessibility of labile N in Arctic ecosystems but our findings indicate the potential for increased accessibility from the mobilization of labile N in the presence of topographic relief and precipitation. A detailed overview of the isotopic analyses performed and results are presented in the Supplemental online material, however, it is worth noting that the $\delta^{15}N$ and $\delta^{18}O$ of soil pore water were consistent with the predicted range of NO_3^- produced through microbial degradation of N-rich alder shrub organic matter. Enrichment of both $\delta^{15}N$ and $\delta^{18}O$ isotopes at wetter downslope locations indicate that denitrification limits the mobility of NO_3^-N by transforming it to other N-species.

4.2 Effects of precipitation on pore water nitrate

Previous studies have linked nutrient flushing with rainfall events (Bechtold et al., 2003; Baldwin and Mitchell, 2000), and several studies have proposed that soil NO_3^- inputs from mineralized and nitrified leaf litter are mobilized at wet-season onset (Yamashita et al., 2010; Bernal et al., 2003). In particular, Vink et al., (2007) found that in a forested catchment, inorganic N accumulated within soil and leaf litter during dry periods and was subsequently flushed into headwater streams during precipitation events – an initial pulse in NO_3^--N in soil pore water quickly declined following increased precipitation and discharge. The dynamic short-term temporal variability of NO_3^--N observed along the A1 transect (Fig 3; within and downslope of shrubland) associated with precipitation events in July and September of 2017 provides evidence that a similar model of NO_3^- accumulation and subsequent mobilization occurs on the KG Hillslope. A 'pulse-like' signal of elevated soil pore water NO_3^--N was observed within and downslope of shrubland along the A1 transect (Fig. 3a) that corresponded to a precipitation event which occurred overnight between July 17 – 18, 2017. This event is reflected in the $\delta^{18}O$ - NO_3^- of two samples collected within shrubland along the A1 transect during this time period, where enriched values of $\delta^{18}O$ (> 10.0 ‰; Fig. S2 in Supplemental material) may indicate a minor influence by atmospheric deposition of NO_3^-.

Rainfall occurred during sampling on all three days of the September 2017 campaign (9/14/17 through 9/16/17; personal observation; Western Regional Climate Center, 2017). During July 2018 (July 22-27) and September 2018 (September 21-22) campaigns, weather conditions were much drier (no recorded precipitation events) and NO_3^--N concentrations showed little variation with no daily pattern, ranging from 4.09 mg L^{-1} to 4.94 mg L^{-1} downslope of shrubland along the A1 transect over the five days in July 2018 and from 0.02 mg L^{-1} to 0.12 mg L^{-1} over two days in September 2018. While the precipitation events in July 2017 and September 2017 did appear to mobilize NO_3^- from the shrubland to the lowland area (down gradient) along the A1 transect, this mobility was only observed within the first 10-30 m downslope of the shrubland (Fig. 4a), indicating the presence of additional controls (such as denitrification bacteria, assimilation, and hydrologic flushing) acting on NO_3^- transport across the landscape.

Deleted: ¶

Deleted: On the KG Hillslope, isotopic signatures of NO_3^- from all but two collections fall within the expected range of $\delta^{18}O$ - NO_3^- of microbially derived NO_3^- (Fig. 5), further indicating that the soil pore water NO_3^- is a product of microbial mineralization and nitrification rather than atmospheric deposition (Schimel and Bennett, 2004). To determine the range of $\delta^{18}O$-NO_3^- derived from microbial nitrification, we used Eq. (1). However, other studies suggest that $\delta^{18}O$-NO_3^- should more closely represent $\delta^{18}O$-H_2O (Boshers et al., 2019). We determined the range of $\delta^{18}O$-NO_3^- derived by microbial nitrification to include both possibilities, shown in Fig. 5. If the source of NO_3^- was by atmospheric deposition, values of $\delta^{15}N$ between ~ -15 ‰ and ~ +15 ‰ and $\delta^{18}O$ between ~ +60 ‰ and ~ +94 ‰ would be expected (Granger and Wankel, 2016). ¶
¶
In September 2017 and September 2018, some samples collected within the shrubland along the A1 and A4 transects had light $\delta^{15}N$-NO_3^- (< -8.0 ‰; Fig. S2 in Supplementary Material). These values are likely representative of nitrification of DON derived from non-alder sources (Fig. 5; more details in Supplementary Material). For example, measurements of leaf $\delta^{15}N$ from moss, lichen, and dwarf shrubs growing upslope from the alder shrublands at the KG Hillslope range from -13.78 ‰ to -8.45 ‰ (Salmon et al., 2019b). Nitrogen from these plant types may have been mobilized downslope from the alder shrubland, resulting in the depleted $\delta^{15}N$ found within our samples. ¶

Deleted: 5

Deleted: ¶

Deleted: This precipitation may be partially reflected in the isotopic composition of water samples collected in September 2017, which had an average $\delta^{18}O$ value of -15.6 ± 0.8 ‰; ~1 ‰ more enriched than water samples collected in July 2017, July 2018, and September 18 ($p<0.001$; Fig. 6 and Table S7 in Supplementary Material).

Deleted: ¶

Deleted: The $\delta^{18}O$ and $\delta^{2}H$ signature of soil pore water approximated the global meteoric water line both in the upland soils ($r^2 = 0.92$) and lowland soils ($r^2 = 0.81$) and indicate that evaporation was negligible during sampling (Fig. S3 in Supplementary Material).

Deleted: Soil pore water in the upland area was heavier in $\delta^{18}O$ composition (-15.62 ± 0.86 ‰) than in the lowland area (-16.56 ± 0.48 ‰), though these ranges overlap (0.40 ‰; Fig. S3 in Supplementary Material). The steep slopes in the upland area also promote prompt drainage of rainfall and active layer melt towards the lowlands, where the transition to a lower gradient, lack of evaporation, and limited vertical drainage result in increased residence times and increased storage capacity. Therefore, soil pore water from the lowland active layer may have had a greater component of isotopically lighter and older spring rainfall/snowmelt and active layer ice melt, while the upland area reflected isotopically enriched, younger summer rainfall relative to our sampling campaigns (Kendall and McDonnell, 1998). Active layer ice in the less well-drained lowland areas would therefore also be expected to be lighter and to contribute more to the isotopic mass balance than in the upland area. Thus, the isotopic composition of water in upland soils likely reflects a larger summer rainfall component while lowland soils likely reflect isotopically lighter active layer ice melt (Throckmorton et al., 2015; Craig, 1961).

4.3 Effects of redox on pore water nitrate-N

The decrease in soil pore water NO_3^--N along the A1 and A4 transects and increase in soil moisture, Fe^{2+}, and Mn along the A4 transect in July 2018 (Fig. 4) and September 2018 (Tables S5, S6, in Supplemental material) indicate a transition from an oxic environment towards a more sub-oxic environment as the slope transitions from upland to lowland. The lack of variation in SO_4^{-2} across these transects indicates that conditions were not reducing enough for sulfate reduction or methanogenesis (Jakobsen and Postma, 1999). Our data indicate that the oxic environment on the well-drained upland slope supports NO_3^--N production while sub-oxic environment of the poorly drained lowland area supports the reduction or denitrification of NO_3^- (Table S5 in Supplemental material).

Callahan et al., (2017) described upland hillslope alders as 'hotspots' for NO_3^- inputs into streams at the hillslope scale, and Harms and Jones (2012) observed greater NO_3^- export in soils with increased active layer thickness. These predictions are consistent with the elevated NO_3^--N concentrations within and directly downslope of alder shrubland along each transect (Fig. 4). The prevailing sub-oxic conditions downslope of A1 and A4 and overall scarcity of inorganic N likely restrict NO_3^- production, indicating that elevated NO_3^--N concentrations observed at these locations was produced within the alder shrubland patches and flushed downslope. However, mobility of NO_3^- beyond the first 20-30 m downslope of shrubland along the A1 and A4 transects was not observed (Fig. 4). Inputs and subsequent dilution from flow along the gradient may be responsible for the decrease in NO_3^--N, but it is more likely due to denitrification occurring in the sub-oxic conditions, as evidenced by the isotopic denitrification trend observed (see Supplemental material for full isotopic discussion). Consistent with these results, a study by Harms and Ludwig (2016) predicted that saturated soils and reducing conditions may buffer N export to downslope ecosystems. Thus, while hillslopes dominated by alder will likely increase NO_3^- availability with shrubification, sub-oxic to reducing zones and soil saturation occurring at downslope locations may serve as buffers to down gradient mobility of NO_3^- through microbial denitrification. Defining the role of topographically controlled redox environments on nutrient cycling in permafrost environments will be beneficial for understanding the likelihood of NO_3^- mobilization to streams and subsequent transport down-gradient within N-limited landscapes.

4.4 Spatial and temporal variations in nitrate-N

Over the limited time series we collected in the 2017 and 2018 growing seasons, significant ($p < 0.05$; Supplemental material) spatiotemporal variability of soil pore water NO_3^--N concentrations were observed at our continuous permafrost site with a distinct ridge-toe slope topography. Spatial variability existed within individual shrubland areas as well as from one shrubland area to another (Fig. 2; Table S5 in Supplemental material). These spatial differences encompassed both changes in the distribution of NO_3^--N within alder shrubland and changes in the magnitude of NO_3^--N present in the landscape over time. Temporally, we observed dynamic daily variability in NO_3^--N correlated with precipitation events at locations within and downslope of an alder shrubland patch (Fig. 3).

Deleted: Supplementary
Deleted: Material
Deleted: that are
Deleted: ¶
In a reducing environment, enrichment of $\delta^{15}N$ and $\delta^{18}O$ occurs during the process of microbial denitrification (Böttcher et al., 1990). In freshwater systems, this enrichment is typically expressed as a 1:1 ($\delta^{18}O$/ $\delta^{15}N$) relationship, though many systems have trajectories greater or less than 1 (Boshers et al., 2019). Deviations from a trajectory of 1 may be a result of nitrification and/or annamox (anaerobic ammonium oxidation) that produces NO_3^- concurrently during denitrification in anoxic conditions (Granger and Wankel, 2016). The locations downslope of alder shrublands follow a similar trend of enrichment in $\delta^{15}N$ and $\delta^{18}O$ with an apparent regression slope of 0.84 (Fig. 5), suggesting denitrification occurring in the lowland areas.¶
Deleted: ry
Deleted: M
Deleted: a
Deleted: ry
Deleted: M

Although soil pore water NO_3^--N was elevated during dry conditions and active drainage through-flow was observed in open soil pits, the notable day-to-day changes in NO_3^--N during wet conditions indicate that this variability was driven primarily by the presence of rainfall. Evidence for this mechanism was observed during or following precipitation events; first after the isolated precipitation event in July 2017 where NO_3^--N concentrations were elevated both within and downslope of alder shrubland in one location (Fig. 3a), and again in September 2017 where NO_3^--N concentrations were elevated downslope but not within the same shrubland (Fig. 3b). On the KG Hillslope, NO_3^- likely accumulates in the soil below alders as litter decomposes (supported by isotopic evidence presented in Supplemental material) and gets mobilized down-gradient with the onset of rainfall. These spatial variations associated with rainfall likely indicate a 'flushing' down gradient of previously accumulated soil NO_3^- from within the alder shrubland and highlight the capacity for NO_3^- to be mobilized across landscapes.

4.5 Future research

Findings from this study illuminate a level of complexity in N cycling that is not widely published by providing snapshots of variability and mobility of NO_3^- on the KG Hillslope over brief time series. Future studies would benefit from the additional incorporation of continuous monitoring of NO_3^- throughout a growing season, consideration of alder characteristics (biomass, root and nodule density, rates of N fixation; Salmon et al., 2019a-b), and targeted transects throughout a permafrost alder landscape (as done in this study) to further characterize spatial variation in soil pore water NO_3^- in relation to alder stand proximity. Studies to further identify processes controlling the availability, transport, and fate of N in permafrost landscapes would benefit from the inclusion of N sources, total N input, organic carbon, microbial community function, and C:N relationships, such as those conducted by Ramm et al. (2020). Long-term impacts of NO_3^- on vegetation, permafrost degradation, and interstitial water chemistry in wet downslope permafrost landscapes also require further investigation. Moreover, identification of microbial communities in the sub-oxic reducing downslope environments would lend insights towards the fate of NO_3^-, whether it is assimilated by plants or reduced to N_2 or nitrous oxide gas.

Furthermore, the dynamic variability of NO_3^--N across the KG Hillslope indicates the importance of improving the representation of N cycle processes in ESMs. Although plant functional types (PFTs) are included in ESMs currently, processes such as N-fixation remain underrepresented in these classifications (Wullschleger et al., 2014), and their incorporation to ESMs could improve nutrient availability and variability predictions.

5 Conclusion

Teasing apart the dynamics between alder shrubland communities, topography, permafrost, and NO_3^- availability is complex because interactions between these factors vary both across time and space. The high degree of NO_3^--N variability observed over short timescales (days) and distances (meters) is documented in this study. The existence of a topographic gradient within our alder shrubland landscape allows for precipitation events to mobilize nitrate downslope. However, redox environments

Deleted: well understood

Deleted: and provides a framework for future research in this topic. Here we

Deleted: e

Deleted: Continuous

Deleted: and

Deleted: replication of this type of study are required to further

Deleted: within individual alder patches

Deleted: should

Deleted: incl

Deleted: ude

Deleted: widespread, comprehensive investigations of

Deleted: being

Deleted: ,

Deleted: Future research should also emphasize the importance of characterizing N cycling to better constrain how storage and release of C will shift with climate warming in the Arctic.

Deleted: studies

Deleted: Lastly,

Deleted:

Deleted: downslope

Deleted: will

Deleted: T

Deleted: demonstrates

Deleted: Including N and C ecological interactions in these models will decrease the uncertainty associated with forecasting atmospheric CO_2 concentrations in a warming climate (Thornton et al., 2009) and bolster increase the predictive power of future models.

Deleted: . This study has shown the importance of incorpor ... [3]

Deleted: N-fixing shrubs in ESMs

Deleted: tens of

Deleted: has not been

Deleted: outside

Deleted: However,

Deleted: we have determined that the fixation of N within ... [4]

Deleted: exists

Deleted: an

Deleted: ,

Deleted: have the potential

Deleted: Nitrate present in soil within alder shrubland is lik ... [5]

Deleted: .

Deleted: however

driven by hillslope topography are important factors in limiting the spatial extent of NO_3^- mobility across permafrost landscapes. These findings have implications for the anticipated nutrient responses associated with the expansion of shrub vegetation in the Arctic and demonstrate the importance of incorporating factors such as topography, redox conditions, and plant functional type in watershed scale studies. Along with permafrost thaw (Harms and Jones, 2012) and changes in soil moisture distribution (Heikoop et al., 2015), the expansion of N-fixing shrubs across tundra landscapes is a dominant mechanism that could greatly increase local NO_3^- availability in the Arctic. However, this study demonstrates that to fully account for the impact of shrubification on NO_3^- availability and export, scientists should also consider topographic gradients, hydrologic conditions, and the presence of geochemical reducing zones that may affect NO_3^- fate and transport.

Data Availability. The complete data set for this research can be accessed at https://doi.org/10.5440/1544760.

Author Contributions. REM, CAA, BDN, JMH, VGS, and CJW conceptualized the study. REM, CAA, BDN, JMH, VGS, SS, and NAW contributed to the study investigation. REM, CAA, BDN, VGS, and JMH performed formal analyses of the data. REM, CAA, BDN, JMH, GBP, and OCM contributed to data curation of this project. CJW and SDW were involved in funding acquisition, project administration, supervision, and resource access. JMH, GBP and OCM provided laboratory resources for this project. REM, CAA, BDN, VGS, and JMH were involved in visualization, the writing of the original draft preparation and the review and editing process. CJW, SS, NAW, and SDW contributed to writing review and editing.

Competing Interests. The authors declare they have no conflicts of interest.

Acknowledgements. This research was completed with oversight and support of the Next-Generation Ecosystems Experiments (NGEE Arctic) project. NGEE Arctic is supported by the Office of Biological and Environmental Research in the U.S. Department of Energy – Office of Science. Support for this research was also provided by the Earth and Environmental Sciences Division at Los Alamos National Laboratory (LANL), the Geological Society of America, and the Marine, Earth, and Atmospheric Sciences (MEAS) Department at North Carolina State University. We would like to thank Mary's Igloo Native Corporation for their guidance and for allowing us to conduct this research on the traditional homelands of the Iñupiat people. We would like to thank Nate Conroy, Emma Lathrop, Emily Kluk, Dea Musa, and the staff at the Geochemistry and Geomaterials Research Laboratory at LANL for their assistance in fieldwork, laboratory analysis, and data organization. We thank Bob Busey for access to continuous weather data. Thank you to the entire NGEE Arctic team for their support. Finally,

Deleted: buffering

Deleted: historic and projected

Deleted: and has implications for water quality and overall ecosystem health

Deleted: This

Deleted: production

Deleted: and accurately represent these dynamics in Earth System Models,

Deleted: include N-fixers as an independent plant functional type, and

Deleted: and

Deleted: gradients

we would like to thank Ethan Hyland and Gwen Hopper for laboratory assistance in the MEAS Department at North Carolina State University.

References

Baldwin, D. S., and Mitchell, A. M.: The effects of drying and re-flooding on the sediment and soil nutrient dynamics of lowland river-floodplain systems: A synthesis, Regul. Rivers: Res. Mgmt., 16, 457–467, https://doi.org/10.1002/1099-1646(200009/10)16:5<457::AID-RRR597>3.3.CO;2-B, 2000.

Barnes, R. T., Williams, M. W., Parman, J. N., Hill, K., and Caine, N.: Thawing glacial and permafrost features contribute to nitrogen export from Green Lakes Valley, Colorado Front Range, USA, Biogeochemistry, 117, 413–430, https://doi.org/10.1007/s10533-013-9886-5, 2014.

Bechtold, J. S., Edwards, R. T., and Naiman R. J.: Biotic versus hydrologic control over seasonal nitrate leaching in a floodplain forest, Biogeochemistry, 63, 53–72, https://doi.org/10.1023/A:1023350127042, 2003.

Bernal, S., Butturini, A., Nin, E., Sabater, F., and Sabater, S.: Leaf litter dynamics and nitrous oxide emission in a Mediterranean riparian forest, J. Environ. Qual., 32, 191–197, https://doi.org/10.2134/jeq2003.1910, 2003.

Boike, J., Juszak, I., Lange, S., Chadburn, S., Burke, E., Overduin, P. P., and Westermann S.: A 20-year record (1998–2017) of permafrost, active layer and meteorological conditions at a high Arctic permafrost research site (Bayelva, Spitsbergen), Earth Syst. Sci. Data, 10, 355–390, https://doi.org/10.5194/essd-10-355-2018, 2018.

Brown, C. E.: Coefficient of Variation, in: Applied multivariate statistics in geohydrology and related sciences, edited by: Brown, C. E., Springer, Berlin, Heidelberg, Germany, 155–157, https://doi.org/10.1007/978-3-642-80328-4_13, 1998.

Bühlmann, T., Hiltbrunner, E., and Körner, C.: *Alnus viridis* expansion contributes to excess reactive nitrogen release, reduces biodiversity and constrains forest succession in the Alps, Alp. Bot., 124, 187–191, https://doi.org/10.1007/s00035-014-0134-y, 2014.

Callahan, M. K., Whigham, D. F., Rain, M. C., Rains, K. C., King, R. S., Walker, C. M., Maurer, J. R., and Baird, D. J.: Nitrogen subsidies from hillslope alder stands to streamside wetlands and headwater streams, Kenai Peninsula, Alaska, JAWRA, 53, 478–492, https://doi.org/10.1111/1752-1688.12508, 2017.

Chapin, F. S., McGraw, J. B., and Shaver, G. R. Competition causes regular spacing of alder in Alaskan shrub tundra. Oecologia 79, 412–416, https://doi.org/10.1007/BF00384322, 1989.

Deleted: Boshers, D. S., Granger, J., Tobias, C. R., Böhlke, J. K., and Smith, R. L.: Constraining the oxygen isotopic composition of nitrate produced by nitrification, Environ. Sci. and Technol., 53, 1206–1216, https://doi.org/10.1021/acs.est.8b03386, 2019.¶
Böttcher, J., Strebel, O., Voerkelius, S., and Schmidt, H. L.: Using isotope fractionation of nitrate-nitrogen and nitrate-oxygen for evaluation of microbial denitrification in a sandy aquifer, J. Hydrol., 114, 413–424, https://doi.org/10.1016/0022-1694(90)90068-9, 1990.¶

Formatted: Font: Italic

Deleted: Casciotti, K. L., Sigman, D. M., Hastings, M. G., Böhlke, J. K., and Hilkert, A.: Measurement of the oxygen isotopic composition of nitrate in seawater and freshwater using the denitrifier method, Anal. Chem., 74, 19, 4905–4912, https://doi.org/10.1021/ac020113w, 2002.¶

Chapin, F. S., Mcguire, A., D., Randerson, J., Pielke, R., Baldocchi, D., Hobbie, S. E., Roulet, N., Eugster, W., Kasischke, E., Rastetter, E. B., Zimov, A., and Running, S. W.: Arctic and boreal ecosystems of western North America as components of the climate system, Glob. Chang. Biol., 6, 211–223, https://doi.org/10.1046/j.1365-2486.2000.06022.x, 2000.

Darrouzet-Nardi, A., and Weintraub, M. N.: Evidence for spatially inaccessible labile N from a comparison of soil core extractions and soil pore water lysimetry, Soil Biol. Biochem., 73, 22–32, https://doi.org/10.1016/j.soilbio.2014.02.010, 2014.

Frost, G. V., Epstein, H. E., Walker, D. A., Matyshak, G., and Ermokhina, K. Patterned-ground facilitates shrub expansion in Low Arctic tundra. Environ. Res. Lett. 8, 015035. https://doi.org/10.1088/1748-9326/8/1/015035, 2013.

Frost, G. V., and Epstein, H. E.: Tall shrub and tree expansion in Siberian tundra ecotones since the 1960s, Glob. Chang. Biol., 20, 1264–1277, https://doi.org/10.1111/gcb.12406, 2014.

Harms, T. K., and Jones, J. B.: Thaw depth determines reaction and transport of inorganic nitrogen in valley bottom permafrost soils, Glob. Chang. Biol., 18, 2958–2968, https://doi.org/10.1111/j.1365-2486.2012.02731.x, 2012.

Harms, T. K., and Ludwig, S. M.: Retention and removal of nitrogen and phosphorus in saturated soils of Arctic hillslopes, Biogeochemistry, 127, 291–304, https://doi.org/10.1007/s10533-016-0181-0, 2016.

Harms, T. K., Cook, C. L., Wlostowski, A. N., Gooseff, M. N., and Godsey, S.E.: Spiraling down hillslopes: nutrient uptake from water tracks in a warming Arctic, Ecosystems, 22, 1546–60, https://doi.org/10.1007/s10021-019-00355-z, 2019.

Heikoop, J. M., Throckmorton, H. M., Newman, B. D., Perkins, G. B., Iversen, C. M., Chowdhury, T. R., Romanovsky, V., Graham, D. E., Norby, R. J., Wilson, C. J., and Wullschleger, S. D.: Isotopic identification of soil and permafrost nitrate sources in an Arctic tundra ecosystem, J. Geophys. Res. Biogeosci., 120, 1000– 1017, https://doi:10.1002/2014JG002883, 2015.

Helsel, D. R., and Hirsch, R. M.: Statistical methods in water resources: Techniques of water resources investigations, 04-A3, U.S. Geological Survey, Reston, VA, USA, 118-122, https://doi:10.3133/twri04A3, 2002.

Hiltbrunner, E., Aerts, R., Bühlmann, T., Huss-Danell, K., Magnusson, B., Myrold, D. D., Reed, S. C., Sigurdsson, B. D., and Körner, C.: Ecological consequences of the expansion of N2-fixing plants in cold biomes, Oecologia, 176, 11–24, https://doi.org/10.1007/s00442-014-2991-x, 2014.

Hinzman, L. D., Deal, C. J., McGuire, A. D., Mernild, S. H., Polyakov, I. V., and Walsh, J. E.: Trajectory of the Arctic as an integrated system, Ecol. Appl., 23, 1837–1868, https://doi.org/10.1890/11-1498.1, 2013.

Deleted: Craig, H.: Isotopic Variations in Meteoric Waters, Science, 133, 1702-1703, http://doi:10.1126/science.133.3465.1702, 1961.¶

Deleted: Granger, J., and Wankel, S. D.: Isotopic overprinting of nitrification on denitrification as a ubiquitous and unifying feature of environmental nitrogen cycling, PNAS, 113, 42, E6391-E6400, https://doi:10.1073/pnas.1601383113, 2016.¶

Deleted: a

Hopkins, D. M., Karlstrom, T. N. V.: Permafrost and groundwater in Alaska, 264-F, US Government Printing Office, United States, Washington D. C., 122-124, 1955.

Hovelsrud, G. K., Poppel, B., van Oort, B., and Reist, J. D.: Arctic societies, cultures, and peoples in a changing cryosphere, AMBIO, 40, 100–110, https://doi.org/10.1007/s13280-011-0219-4, 2011.

Hurd, T. M., and Raynal, D. J.: Comparison of nitrogen solute concentrations within alder (Alnus incana ssp. rugosa) and non-alder dominated wetlands, Hydrol. Process., 18, 2681–2697, https://doi.org/10.1002/hyp.5575, 2004.

Iversen, C., Breen, A., Salmon, V., Vander Stel, H., and Wullschleger, S. D.: NGEE Arctic Plant Traits: Vegetation plot locations, ecotypes, and photos, Kougarok Road mile marker 64, Seward Peninsula, Alaska, 2016, Next Generation Ecosystem Experiments Arctic [data set], https://doi:10.5440/1346196, 2016.

Jakobsen, R. and Postma, D.: Redox zoning, rates of sulfate reduction and interactions with Fe-reduction and methanogenesis in a shallow sandy aquifer, Rømø, Denmark, Geochim. Cosmochim. Acta, 63, 137-151, https://doi.org/10.1016/S0016-7037(98)00272-5, 1999.

Ju, J., and Masek, J. G.: The vegetation greenness trend in Canada and US Alaska from 1984–2012 Landsat data, Remote Sens. Environ., 176, 1-16, https://doi.org/10.1016/j.rse.2016.01.001, 2016.

Keuper, F., Dorrepaal, E., van Bodegom, P. M., van Logtestijn, R., Venhuizen, G., van Hal, J., and Aerts, R.: Experimentally increased nutrient availability at the permafrost thaw front selectively enhances biomass production of deep-rooting subarctic peatland species, Glob. Change Biol., 23, 4257–4266, https://doi.org/10.1111/gcb.13804, 2017.

Koch, J. C., Runkel, R. L., Striegl, R., and McKnight, D. M.: Hydrologic controls on the transport and cycling of carbon and nitrogen in a boreal catchment underlain by continuous permafrost, J. Geophys. Res.: Biogeosci., 118, 698–712, https://doi.org/10.1002/jgrg.20058, 2013.

Martin, P. D., Jenkins, J. L., Adams, F. J., Torre, M., Matz, A. C., Payer, D. C., Reynolds, P. E., Tidwell, A. C., and Zelenak, J. R.: Wildlife response to environmental Arctic change: Predicting Future Habitats of Arctic Alaska, report from: The Wildlife Response to Environmental Arctic Change (WildREACH): Predicting future habitats of Arctic Alaska workshop, Fairbanks, AK, USA, 17-18 November 2008.

McClelland, J. W., Stieglitz, M., Pan, F., Holmes, R. M., and Peterson, B. J.: Recent changes in nitrate and dissolved organic carbon export from the upper Kuparuk River, North Slope, Alaska: N and C export from the Kuparuk River, J. Geophys. Res.: Biogeosci., 112, G4, https://doi.org/10.1029/2006JG000371, 2007.

Deleted: Kendall, C., and McDonnell, J. J. (Eds.): Isotope tracers in catchment hydrology, Elsevier Science B.V., Amsterdam, 519-576, https://doi.org/10.1016/C2009-0-10239-8, 1998.¶

Mitchell, J. S., and Ruess, R. W.: N2 fixing alder (*Alnus viridis* spp. *fruticosa*) effects on soil properties across a secondary successional chronosequence in interior Alaska, Biogeochemistry, 95, 215–229, https://doi.org/10.1007/s10533-009-9332-x, 2009.

Moatar, F., Abbot, B. W., Minaudo, C., Curie, F., Pinay, G.: Elemental properties, hydrology, and biology interact to shape concentration-discharge curves for carbon, nutrients, sediment, and major ions. Water Resour. Res., 53: 1270-1287, https://doi.org/10.1002/2016WR019635, 2017.

Myers-Smith, I. H., Forbes, B. C., Wilmking, M., Hallinger, M., Lantz, T., Blok, D., Tape, K. D., Macias-Fauria, M., Sass-Klaassen, U., and Lévesque, E.: Shrub expansion in tundra ecosystems: dynamics, impacts and research priorities, Environ. Res. Lett., 6, 045509, https://doi.org/10.1088/1748-9326/6/4/045509, 2011.

Myers-Smith, I. H., Elmendorf, S. C., Beck, P. S. A., Wilmking, M., Hallinger, M., Blok, D, Tape, K. D., Rayback, S. A., Macias-Fauria, M., Forbes, B. C., Speed, J. D. M., Boulanger-Lapointe, N., Rixen, C., Lévesque, E., Schmidt, N. M., Baittinger, C., Trant, A. J., Hermanutz, L., Collier, L. S., Dawes, M. A., Lantz, T. C., Weijers, S., Jørgensen, R. H., Buchwal, A., Buras, A., Naito, A. T., Ravolainen, V., Schaepman-Strub, G., Wheeler, J. A., Wipf, S., Guay, K. C., Hik, D. S., and Vellend, M.: Climate sensitivity of shrub growth across the tundra biome, Nat. Clim. Chang., 5, 887–891, https://doi.org/10.1038/nclimate2697, 2015.

O'Donnell, J. A., and Jones, J. B.: Nitrogen retention in the riparian zone of catchments underlain by discontinuous permafrost, Freshw. Biol., 51, 854–864, https://doi.org/10.1111/j.1365-2427.2006.01535.x, 2006.

Ogawa, A., Shibata, H., Suzuki, K., Mitchell, M. J., and Ikegami, Y.: Relationship of topography to surface water chemistry with particular focus on nitrogen and organic carbon solutes within a forested watershed in Hokkaido, Japan, Hydrol. Process., 20, 251–265, https://doi.org/10.1002/hyp.5901, 2006.

Racine, C. H. Flora and vegetation: Biological Survey of the Proposed Kobuk Valley National Monument. Final Report ed H. R. Melchior (Fairbanks, AK: Alaska Cooperative Park Studies Unit, Biology and Resource Management Program, University of Alaska) pp 39–139, 1976.

Racine, C. H. and Anderson, J. H. Flora and vegetation of the Chukchi-Imuruk area Biological Survey of the Bering Land Bridge National Monument: Revised Final Report ed H. R. Melchior (Fairbanks, AK: Alaska Cooperative Park Studies Unit, Biology and Resources Management Program, University of Alaska) pp 38–113, 1979.

Ramm, E., Liu, C., Wang, X., Yue, H., Zhang, W., Pan, Y., Schloter, M., Gschwendtner, S., Mueller, C. W., Hu, B., Rennenberg, H., and Dannenmann, M.: The forgotten nutrient - The role of nitrogen in permafrost soils of Northern China, Adv. Atmos. Sci., 37, 793-799, https://doi.org/10.1007/s00376-020-0027-5, 2020.

Formatted: Font: Italic

Formatted: Font: Italic

Deleted: ¶

Rhoades, C., Óskarsson, H., Binkley, D., and Stottlemyer, R.: Alder (Alnus crispa) effects on soils in ecosystems of the Agashashok River valley, northwest Alaska, Ecoscience, 8, 89-95, https://doi.10.1080/11956860.2001.11682634, 2001.

Romanovsky, V. E., and Osterkamp, T. E.: Effects of unfrozen water on heat and mass transport processes in the active layer and permafrost, Permafrost Periglac., 11, 219–239. https://doi.org/10.1002/1099-1530(200007/09)11:3<219::AID-PPP352>3.0.CO;2-7, 2000.

Roy, S., Khasa, D. P., and Greer, C. W.: Combining alders, frankiae, and mycorrhizae for the revegetation and remediation of contaminated ecosystems, Can. J. Bot., 85, 237–251, https://doi.org/10.1139/B07-017, 2007.

Salmon, V. G., Soucy, P., Mauritz, M., Celis, G., Natali, S. M., Mack, M. C., and Schuur, E. A. G.: Nitrogen availability increases in a tundra ecosystem during five years of experimental permafrost thaw, Glob. Chang. Biol., 22, 1927-1941, https://doi:10.1111/gcb.13204, 2016.

Salmon, V. G., Breen, A. L., Kumar, J., Lara, M. J., Thornton, P. E., Wullschleger ,S. D., and Iversen, C. M.: Alder distribution and expansion across a tundra hillslope: Implications for local N cycling, Front. Plant Sci., 10:1099. https://doi:10.3389/fpls.2019.01099, 2019a.

Salmon, V. G., Iversen, C. M., Breen, A. L., Vander Stel, H., and Childs, J.: NGEE Arctic Plant Traits: Plant Biomass and Traits, Kougarok Road Mile Marker 64, Seward Peninsula, Alaska, beginning 2016, Next Generation Ecosystem Experiments Arctic [data set], https://doi.org/10.5440/1346199, 2019b.

Schuur, E. A. G., McGuire, A. D., Schädel, C., Grosse, G., Harden, J. W., Hayes, D. J., Hugelius, G., Koven, C. D., Kuhry, P., Lawrence, D. M., Natali, S. M., Olefeldt, D., Romanovsky, V. E., Schaefer, K., Turetsky, M. R., Treat, C. C., and Vonk, J. E.: Climate change and the permafrost carbon feedback, Nature, 520, 171–179, https://doi.org/10.1038/nature14338, 2015.

Seeberg-Elverfeldt, J., Schlüter, M., Feseker, T., and Kölling, M.: Rhizon sampling of porewaters near the sediment-water interface of aquatic systems, Limn. Oceanogr. Methods, 3, 361–371, https://doi.org/10.4319/lom.2005.3.361, 2005.

Shaftel, R. S., King, R. S., and Back, J. A.: Alder cover drives nitrogen availability in Kenai lowland headwater streams, Alaska, Biogeochemistry, 107, 135–148, https://doi.org/10.1007/s10533-010-9541-3, 2012.

Sharkhuu, N., and Sharkhuu, A.: Effects of climate warming and vegetation cover on permafrost of Mongolia, in: Eurasian Steppes. Ecological Problems and Livelihoods in a Changing World, edited by: Werger, M. J. A., and van Staalduinen, M. A., Springer Netherlands, Heidelberg, Germany, 445–472, https://doi.org/10.1007/978-94-007-3886-7_17, 2012.

Shaver, G. R., and Chapin, F. S.: Response to fertilization by various plant growth forms in an Alaskan tundra: Nutrient accumulation and growth, Ecology, 61, 662–675, https://doi.org/10.2307/1937432, 1980.

Deleted: Schimel, J., and Bennett, J.: Nitrogen mineralization: Challenges of a changing paradigm. Ecology, 85, 591-602, https://doi.org/10.1890/03-8002, 2004.¶

Stookey, L. L.: Ferrozine-A new pectrophotometric reagent for iron, Anal. Chem., 42, 779-781, https://doi: 10.1021/ac60289a016, 1970.

Street, L. E., Burns, N. R., and Woodin, S. J.: Slow recovery of High Arctic heath communities from nitrogen enrichment, New Phytol., 206, 682–695, https://doi.org/10.1111/nph.13265, 2015.

Sturm M., Racine, C., and Tape, K.: Increasing shrub abundance in the Arctic, Nature, 411, 546–547, https://doi.org/10.1038/35079180, 2001.

Sulman, B. N., Salmon, V. G., Iversen, C. M., Breen, A. L., Yuan, F., and Thornton, P. E. Integrating Arctic plant functional types in a land surface model using above- and belowground field observations. J. Adv. Model. 13, e2020MS002396, https://doi.org/10.1029/2020MS002396, 2021.

Tape, K. D., Sturm, M., and Racine, C.: The evidence for shrub expansion in Northern Alaska and the Pan-Arctic, Glob. Chang. Biol., 12, 686–702, https://doi.org/10.1111/j.1365-2486.2006.01128.x, 2006.

Tape, K. D., Hallinger, M., Welker, J. M., and Ruess, R. W.: Landscape heterogeneity of shrub expansion in Arctic Alaska, Ecosystems, 15, 711–724, https://doi.org/10.1007/s10021-012-9540-4, 2012.

Throckmorton, H. M., Heikoop, J. M., Newman, B. D., Altmann, G. L., Conrad, M. S., Muss, J. D., Perkins, G. B., Smith, L. J., Torn, M. S., Wullschleger, S. D., and Wilson, C. J.: Pathways and transformations of dissolved methane and dissolved inorganic carbon in Arctic tundra watersheds: Evidence from analysis of stable isotopes, Global Biogeochem. Cycles, 29, 1893–1910, https://doi:10.1002/2014GB005044, 2015.

Till, A. B., Dumoulin, J. A., Werdon, M. B., and Bleick, H. A.: Bedrock geologic map of the Seward Peninsula, Alaska, and accompanying conodont data, USGS Scientific Investigations Map 3131, 75 pp., 2011.

Vink, S., Ford, P. W., Bormans M., Kelly, C., and Turley, C.: Contrasting nutrient exports from a forested and an agricultural catchment in south-eastern Australia, Biogeochemistry, 84, 247–264, https://doi.org/10.1007/s10533-007-9113-3, 2007.

Vitousek, P. M., Aber, J. D., Howarth, R. W., Likens, G. E., Matson, P. A., Schindler, D. W., Schlesinger, W. H., and Tilman, D. G.: Human alteration of the global nitrogen cycle: Sources and consequences, Ecol. Appl., 7, 737–750, https://doi.org/10.1890/1051-0761(1997)007[0737:HAOTGN]2.0.CO;2, 1997.

Walvoord, M. A., and Kurylyk, B. L.: Hydrologic impacts of thawing permafrost - A review, Vadose Zone J., 15, 1-20, https://doi:10.2136/vzj2016.01.0010, 2016.

Deleted: Sigman, D. M., Casciotti, K. L., Andreani, M., Barford, C., Galanter, M., and Böhlke, J. K.: A bacterial method for the nitrogen isotopic analysis of nitrate in seawater and freshwater, Anal. Chem., 73, 4145–4153, https://doi.org/10.1021/ac010088e, 2001.¶

Deleted: ¶
Thornton, P. E., Doney, S. C., Lindsay, K., Moore, J. K., Mahowald, N., Randerson, J. T., Fung, I., Lamarque, J.-F., Feddema, J. J., and Lee, Y.-H.: Carbon-nitrogen interactions regulate climate-carbon cycle feedbacks: results from an atmosphere-ocean general circulation model, Biogeosciences, 6, 2099–2120, https://doi.org/10.5194/bg-6-2099-2009, 2009.

Weintraub, M. N., and Schimel, J. P.: Interactions between carbon and nitrogen mineralization and soil organic matter chemistry in Arctic tundra soils, Ecosystems, 6, 129–143, https://doi.org/10.1007/s10021-002-0124-6, 2003.

Weintraub, M. N., and Schimel, J. P.: Nitrogen cycling and the spread of shrubs control changes in the carbon balance of Arctic tundra ecosystems, BioScience, 55, 408–415, https://doi.org/10.1641/0006-3568(2005)055[0408:NCATSO]2.0.CO;2, 2005.

Western Regional Climate Center: RAWS USA Climate Archive, retrieved from: https://raws.dri.edu/cgi-bin/rawMAIN.pl?akAQTZ, 2017.

Whigham, D. F., Walker, C. M., Maurer, J., King, R. S., Hauser, W., Baird, S., Keuskamp, J. A., and Neale, P. J.: Watershed influences on the structure and function of riparian wetlands associated with headwater streams - Kenai Peninsula, Alaska, Sci. Total Environ., 599, 124–134, https://doi.org/10.1016/j.scitotenv.2017.03.290, 2017.

Wullschleger, S. D., Epstein, H. E., Box, E. O., Euskirchen, E. S., Goswami, S., Iversen, C. M., Kattge, J., Norby, R. J., van Bodegom, P. M., and Xu, Z.: Plant functional types in Earth system models: past experiences and future directions for application of dynamic vegetation models in high-latitude ecosystems, Ann. Bot., 114, 1–16, https://doi.org/10.1093/aob/mcu077, 2014.

Yamashita, N., Ohta, S., Sase, H., Luangjame, J., Visaratana, T., Kievuttinon, B., and Kanzaki, M.: Seasonal and spatial variation of nitrogen dynamics in the litter and surface soil layers on a tropical dry evergreen forest slope, For. Ecol. Manage., 259, 1502–1512, https://doi.org/10.1016/j.foreco.2010.01.026, 2010.

Yano, Y., Shaver, G. R., Giblin, A. E., Rastetter, E. B., and Nadelhoffer, K. J.: Nitrogen dynamics in a small Arctic watershed: retention and downhill movement of 15N, Ecol. Monogr., 80, 331-351, https://doi:10.1890/08-0773.1, 2010.

Figures

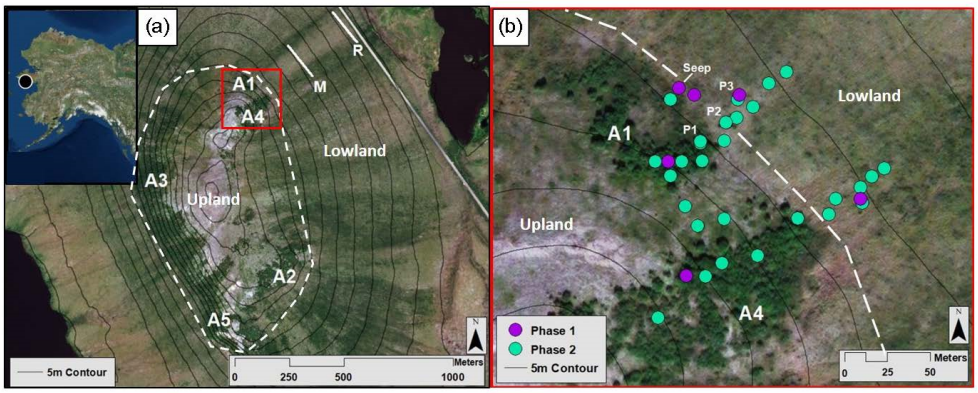

Figure 1: Kougarok Field Site and sampling locations. Upper left inset map with Kougarok Field Site denoted by a black circle, located approximately 80 kilometers inland from the town of Nome on the Seward Peninsula, AK. (a) Alder patch and transect locations at the Kougarok Hillslope. Solid white lines represent Middle (M) and Road (R) sampling transects. Dashed white line represents the boundary between upland area and lowland area. (b) Higher resolution spatial sampling locations within A1 and A4 transects; corresponds to the red box in Fig. 1a. Phase 1 (July 2017) locations are denoted with purple dots. Green dots indicate additional locations sampled during Phase 2 (September 2017, July 2018, and September 2018). P1, P2, and P3 indicate Pit locations dug in July 2018. Dashed white line represents the boundary between upland area and lowland area. Aerial imagery in this figure are sourced from Esri, DigitalGlobe, GeoEye, Earthstar Geographics, CNES/Airbus DS, USDA, USGS, AeroGRID, IGN, and the GIS User Community.

Deleted: (a)
Deleted: is
Deleted: b
Deleted: c
Deleted: 1b

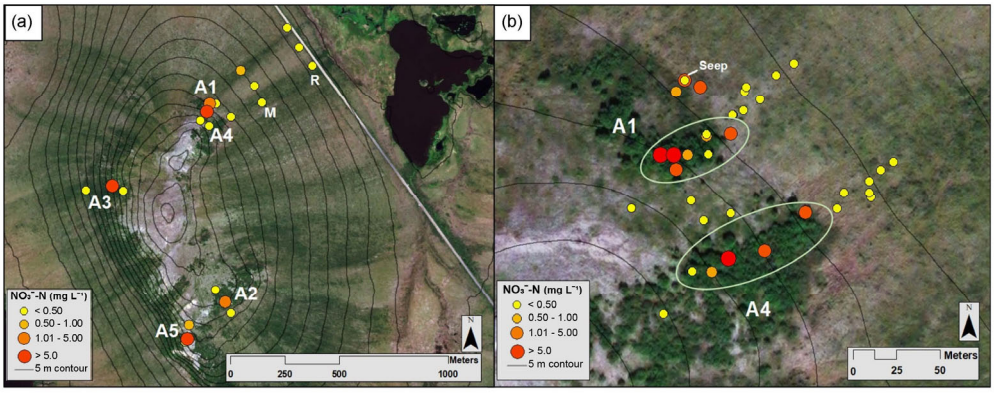

Figure 2: Map of mean NO_3^--N concentrations from the Phase 1 and 2 sampling locations where yellow indicates low concentrations and red indicates high concentrations (see Key for ranges, scales differ slightly). (a) Circles represent NO_3^--N concentrations at locations along the A1–A5, Middle, and Road transects in July 2017. (b) Dots represent average NO_3^--N concentrations along the A1 and A4 transects and between the transects over all sampling campaigns. The green ellipses indicate samples collected *within* the alder shrubland, as opposed to *outside* the alder shrubland. Aerial imagery in this figure are sourced from Esri, DigitalGlobe, GeoEye, Earthstar Geographics, CNES/Airbus DS, USDA, USGS, AeroGRID, IGN, and the GIS User Community.

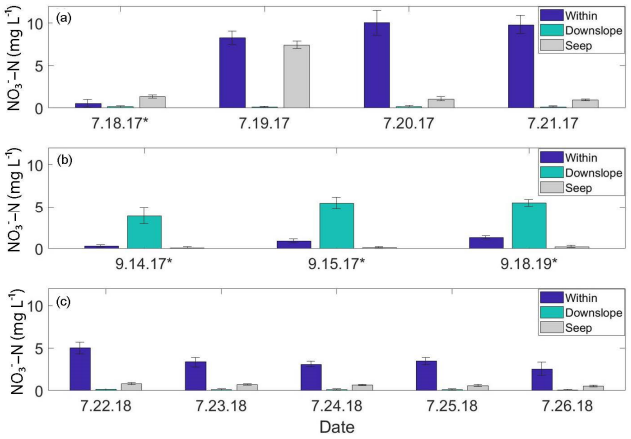

Figure 3: Soil pore water NO_3^--N time series plots from the A1 transect. 'Within' and 'Downslope' denote sample locations within and downslope of shrublands along the transect; 'Seep' denotes a seep in the ground located on the A1 transect at the transition between upland and lowland. Standard deviations are displayed as black brackets on each bar. (a) July 2017 daily NO_3^--N concentrations. (b) September 2017 daily NO_3^--N concentrations. (c) July 2018 daily NO_3^--N concentrations. Days marked with an asterisk (*) indicate precipitation events.

Deleted:

Formatted: Not Superscript/ Subscript

Deleted:

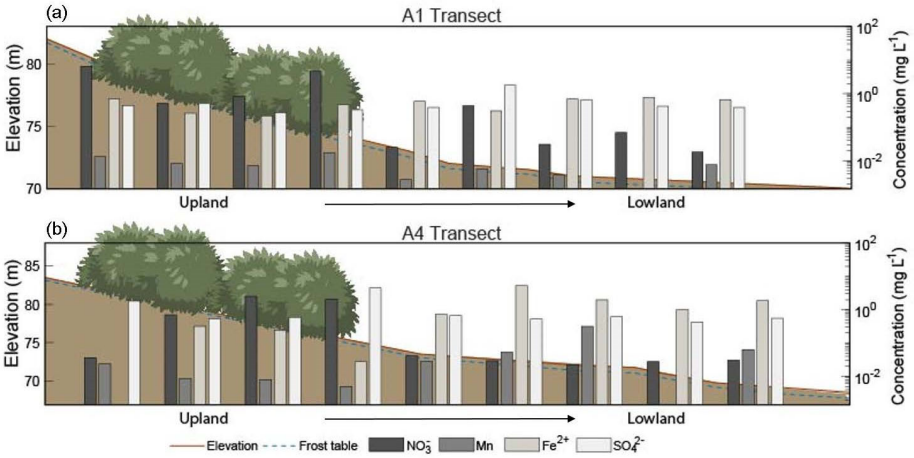

Figure 4: Elevation profiles and chemical concentrations along (a) A1 and (b) A4 transects, extending from the upland area to the lowland area during July (2018) sampling. Note that the elevation scale is different for A1 and A4 transects. Horizontal axis and shrubs not to scale. Depth to frozen soil or bedrock is depicted by the blue dashed line and shrubs indicate sample sites located within the alder shrubland. Redox

species: nitrate (NO_3^--N), manganese (Mn), iron (Fe^{2+}), and sulfate (SO_4^{2-}) are plotted along the secondary y-axis. See Tables S5-S6 in the associated Supplemental material for corresponding concentrations, n-values, and statistics.

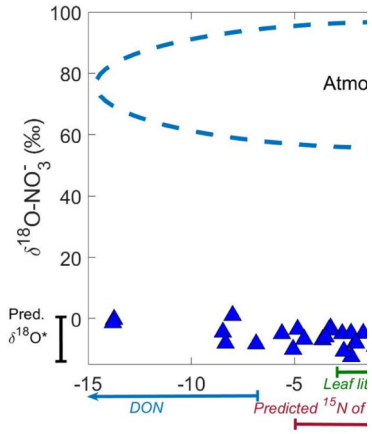

Deleted:
Figure 5: Oxygen ($\delta^{18}O$) versus nitrogen ($\delta^{15}N$) isotopes of soil pore water NO_3^-. Dark blue triangles represent samples within alder shrubland in upland areas. Light blue circles represent samples downslope of alder shrubland in lowland areas. The denitrification process of the downslope samples is denoted by the black arrow inside the plot (y = 0.84x - 7.70). The vertical black line segment (Pred. $\delta^{18}O^*$) denotes the predicted range of $\delta^{18}O$ of NO_3^- produced by microbial nitrification (Eq. 1). The horizontal red line segment indicates the likely $\delta^{15}N$ of NO_3^- range for mineralization and nitrification of organic matter derived from alder material (N-fixation; Kendall and McDonnell, 1998). The likely range of $\delta^{15}N$ of NO_3^- from leaf litter is shown by the horizontal green line segment. The horizontal blue arrow denotes the range of $\delta^{15}N$ of NO_3^- from DON, and the horizontal purple line segment indicates the range of $\delta^{15}N$ of NO_3^- from SON. ¶
¶

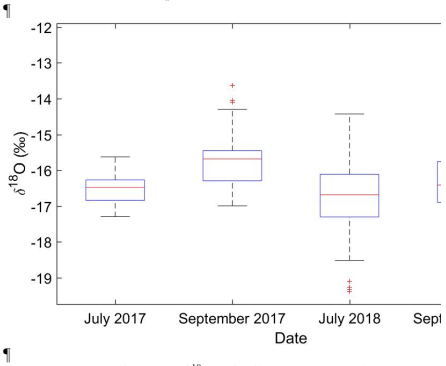

¶
Figure 6: Oxygen isotopes ($\delta^{18}O$) of soil pore water on the KG Hillslope during July and September of 2017 and 2018. The t ... [6]

Formatted: Space After: 0 pt, Line spacing: 1.5 lines

Page 2: [1] Deleted	**Carli A Arendt**	**11/5/2021 1:14:00 PM**
Page 2: [2] Deleted	**Carli A Arendt**	**11/8/2021 1:27:00 PM**
Page 12: [3] Deleted	**Carli A Arendt**	**11/8/2021 2:23:00 PM**
Page 12: [4] Deleted	**Carli A Arendt**	**11/4/2021 2:34:00 PM**
Page 12: [5] Deleted	**Carli A Arendt**	**10/29/2021 4:11:00 PM**
Page 23: [6] Deleted	**Carli A Arendt**	**11/8/2021 9:30:00 AM**